
Efficient and Transferable Adversarial Examples from Bayesian Neural Networks

Martin Gubri¹ Maxime Cordy¹ Mike Papadakis¹ Yves Le Traon¹

Abstract

An established way to improve the transferability of black-box evasion attacks is to craft the adversarial examples on a surrogate ensemble model. Unfortunately, such methods involve heavy computation costs to train the models forming the ensemble. Based on a state-of-the-art Bayesian Neural Network technique, we propose a new method to efficiently build such surrogates by sampling from the posterior distribution of neural network weights during a single training process. Our experiments on ImageNet and CIFAR-10 show that our approach improves the transfer rates of four state-of-the-art attacks significantly (between 2.5 and 44.4 percentage points), in both intra-architecture and inter-architecture cases. On ImageNet, our approach can reach 94% of transfer rate while reducing training time from 387 to 136 hours on our infrastructure, compared to an ensemble of independently trained DNNs. Furthermore, our approach can be combined with test-time techniques improving transferability, further increasing their effectiveness by up to 25.1 percentage points.

1. Introduction

Deep Neural Networks (DNNs) have caught a lot of attention in recent years thanks to their capability to solve efficiently various tasks, especially in computer vision (Dargan et al., 2019). However, a common pitfall of these models is that they are vulnerable to adversarial examples, i.e. misclassified examples that result from slightly altering a well-classified example at test time. For instance, it was shown that adding carefully chosen, elusive perturbations to a correctly classified image may cause misclassification (Biggio et al., 2013; Szegedy et al., 2013). This constitutes a critical security threat for any system embedding DNNs, as

¹Interdisciplinary Centre for Security, Reliability and Trust, University of Luxembourg, Luxembourg. Correspondence to: Martin Gubri <firstname.lastname@uni.lu>.

a malicious third party may exploit this property to enforce some desired outcome.

Such *adversarial attacks* have been primarily designed in white-box settings, where the attacker is assumed to have complete knowledge of the target DNN (incl. its weights). While studying such worst-case scenarios is essential for proper security assessment, in practice the attacker should have limited, or even no knowledge of the target model. In such a case the adversarial attack is applied to a surrogate model, with the hope that the produced adversarial examples *transfer to* (i.e., are also misclassified by) the target DNN.

Achieving transferability remains challenging, though. This is because adversarial attacks were designed to exploit specific information of the surrogate model (e.g., the gradient of its loss function (Goodfellow et al., 2014; Kurakin et al., 2019)), which are different in the target model. As a result, Liu et al. (2017) improved transferability by attacking an *ensemble* of surrogate models. The key intuition is that adversarial examples that fool a diverse set of models are more likely to generalize.

While ensemble-based attacks typically report significantly higher success rates than their single-model counterparts (e.g. Liu et al. (2017)), their computational cost is prohibitive due to the necessity to independently train several surrogate models (to form a diverse ensemble).

In this paper, we propose a new method to improve the transferability of adversarial examples by building diverse ensembles with lesser computation overhead compared to classical ensemble-based methods. Our approach leans upon recent results in approximate inference for Bayesian deep learning. More precisely, we apply a cyclical variant of Stochastic Gradient Markov Chain Monte Carlo (i.e., *cSGLD* (Zhang et al., 2020)) during model training to sample from the posterior distribution on model parameters. This yields a set of models with the same architecture but different weights, which we use to build an ensemble to be attacked. Diversity within the ensemble is achieved thanks to the cyclical nature of cSGLD, whose capability to sample from different modes of the weight posterior distribution has previously been demonstrated (Zhang et al., 2020).

Another advantage of our method is that it requires minimal

modifications of the adversarial attack algorithms and the surrogate model. Thus, it can be applied on top of any attack. We show, moreover, that our approach is complementary to other heuristics to improve transferability.

We evaluate our approach on the CIFAR-10 and the ImageNet datasets (with 5 DNN architectures each), four adversarial attack algorithms and three test-time transformations. Overall, our results indicate that applying cSGLD significantly improves the transfer rate compared to training single DNNs and outperforms classical ensemble-based attacks both in terms of transferability rate and computation cost. Training independent DNNs requires at least 2.42 times more epochs to achieve the same success rates than cSGLD when the targeted architecture is known. This can represent, on ImageNet and our infrastructure, a saving of 251 hours (136 vs 387). At the same computation budget, our method increases the intra-architecture transfer rates between 12.8 and 44.4 percentage points. The inter-architecture transfer rates are increases between 2.5 and 29.2 percentage points at constant computation costs. cSGLD is able to raise the effectiveness of test-time transformations by up to 25.1 percentage points.

To summarize, our contributions are:

- We relate Bayesian inference and transfer-based attacks to propose the first method based on a Bayesian Neural Networks technique to generate transferable adversarial examples. Our approach differs from previous research as it can increase ensemble diversity within a single training process and does not require post-training modification of the surrogate model.
- Our generic method paves the way for improving various adversarial methods by considering the training cost. It applies to any DNN architecture and attack algorithms. Moreover, it is compatible with other heuristics to improve the efficiency and transferability of adversarial attacks (e.g., Liu et al. (2017)).
- Our evaluation on CIFAR-10 and ImageNet reveals significant improvements over the single-DNN and deep ensemble baselines. Compared to classical ensembles trained with the same computation budget, our approach increases transfer rate by up to 44.4 (intra-architecture) and 29.2 (inter-architecture) percentage points.

2. Background and Related work

Adversarial Attacks. We consider 4 gradient-based attacks which aims to maximise the prediction loss $L(x, y, \theta)$ with a p -norm constraint: $\arg \max_{\|\delta\|_p \leq \varepsilon} L(x + \delta, y, \theta)$. FGSM (Goodfellow et al., 2014) is a L_∞ single-step attack defined by $\delta_{\text{FGSM}} = \varepsilon \text{sign}(\nabla_x L(x, y, \theta))$. FGM is

its L2 equivalent: $\delta_{\text{FGM}} = \varepsilon \frac{\nabla_x L(x, y, \theta)}{\|\nabla_x L(x, y, \theta)\|_2}$. The resulting adversarial example is then clipped in $[0, 1]$. I-FGSM (Kurakin et al., 2019) applies iteratively the fast gradient attack with a small step-size α : $\delta_0 = 0$ and $\delta_{i+1} = \text{proj}_{B_\varepsilon}(\delta_i + \alpha \text{sign}(\nabla_x L(x, y, \theta)))$, where $\text{proj}_{B_\varepsilon}(\bullet)$ projects the perturbation in the L_p ball of radius ε . The L2 I-FGM attack is derived similarly. MI-FGSM attack (Dong et al., 2018) adds a momentum term with decay factor μ to the previous attack: $g_{i+1} = \mu g_t + \frac{\nabla_x L(x, y, \theta)}{\|\nabla_x L(x, y, \theta)\|_1}$ and $\delta_{i+1} = \text{proj}_{B_\varepsilon}(\delta_i + \alpha \text{sign}(g_{t+1}))$. PGD (Madry et al., 2018) adds random restarts to I-FG(S)M where each δ_0 is sampled uniformly inside the ball B_ε . The relations between these attacks are illustrated in supplementary materials.

Ensemble Surrogate. Liu et al. (2017) show the benefit of an ensemble surrogate model for inter-architecture black-box attacks. Our work leans on theirs and complement it by demonstrating that attacking models sampled with cSGLD (forming an ensemble from a unique architecture) achieves better transferability at lesser computation cost.

Input and Model Transformations. Other approaches have been developed to improve transferability of adversarial examples. These work at test time (i.e., after training, when performing the attack) and consist of transforming the model or the input. *Ghost Networks* (Li et al., 2018) use Dropout and Skip Connection Erosion to generate on-the-fly diverse sets of surrogate models from one or more base models. *Input Diversity* (Xie et al., 2019) applies random transformations (random resize followed by random padding) to the input images at each attack iteration. *Translation Invariant* (Dong et al., 2019) applies a kernel to the gradient at every attack iteration to optimize over an ensemble of translated images. These techniques can naturally be combined to ours: (i) cSGLD can provide at low computation cost a diverse set of base models to build ghost networks; (ii) Input Diversity and Translation Invariant are attack variants that apply transformations to adversarial inputs independently of the surrogate models. As our evaluation will reveal, our train-time method further improves the transferability of the above three techniques. It is also compatible with other test-time approaches not considered in this paper, such as: linear backpropagation (Guo et al., 2020), intermediate level attack (Huang et al., 2019), Nesterov accelerated gradient and scale invariance (Lin et al., 2019), and serial mini-batch ensemble attack (Che, 2020).

Bayesian Neural Network (BNN) and adversarial examples. Though not our goal, past research aimed at generating adversarial examples for BNNs (we rather use Bayesian deep learning as a way to attack classical DNNs). Grosse et al. (2018) show that BNN uncertainty measures are vulnerable to high-confidence-low-uncertainty adversarial examples transferred from Gaussian Processes. Palacci & Hess

(2018) show that several SG-MCMC sampling schemes are not secure against white-box attack. Wang et al. (2018) used SGLD and Generative Adversarial Network to detect adversarial examples instead of crafting them.

The recent work of Carbone et al. (2020) shows that in the large-data, overparametrized limit for BNN, the gradient of the posterior predictive distribution reaches zero, which makes white-box gradient-based attacks unsuccessful. Our experiments reveal opposite conclusions: our attacks on surrogates DNNs suffer more often from zero gradients than on BNN surrogates. Our settings differs from Carbone et al. (2020) in several aspects: (i) the attacker controls the BNN surrogate and can exploit the cyclical nature of cSGLD to avoid global convergence; (ii) our cheaper SG-MCMC approximation of the posterior predictive distribution (compared to the Hamiltonian Monte Carlo & Variational Inference used in Carbone et al. (2020)) may produce correlated MCMC samples, which explains that the averaged gradient is not zero; (iii) we consider larger datasets (ImageNet and CIFAR-10) than them (MNIST and Fashion-MNIST), where convergence to flat loss is harder to reach.

3. Approach

Transferability in the Bayesian Framework. We consider a classification problem with training dataset $\mathcal{D} = \{(x_i, y_i) \sim p(x, y)\}_{i=1}^N$ and C class labels. A probabilistic classifier parametrised by θ maps x_i into a predictive distribution $\hat{p}(y|x_i, \theta)$. A white-box adversarial perturbation of a test example $(x, y) \sim p(x, y)$ against such classifier is defined as:

$$\delta_\theta = \arg \min_{\|\delta\|_p \leq \varepsilon} \hat{p}(y|x + \delta, \theta).$$

In practice, this optimization problem is solved by replacing the predictive distribution with a loss function (see Section 2). The *transferability* phenomenon was formulated as the empirical observation that an adversarial example for one model is likely to be adversarial for another one (Goodfellow et al., 2014). Black-box attacks can leverage this property by crafting adversarial examples using white-box attacks against a surrogate model to target an unseen model (Papernot et al., 2016).

In black-box setting without oracle access, the targeted classifier is unknown. Assuming that (i) its architecture is known and so is $\hat{p}(y|x, \bullet)$ (we discuss the unknown architecture case further on), (ii) its training set \mathcal{D} is known, (iii) its parameters θ_t are unknown, one can treat θ_t as a random variable s.t. $\theta_t \sim p(\theta|\mathcal{D})$. Then the black-box attack objective is:

$$\delta^* = \arg \min_{\|\delta\|_p \leq \varepsilon} \mathbb{E}_{\theta_t \sim p(\theta|\mathcal{D})} \hat{p}(y|x + \delta, \theta_t). \quad (1)$$

In other words, *the best transferable adversarial example minimizes the true Bayesian posterior predictive distribution* $p(y|x, \mathcal{D}) = \mathbb{E}_{p(\theta|\mathcal{D})} p(y|x, \theta)$. However its closed form is intractable for DNNs.

As previously stated, usually in adversarial learning, transferable adversarial examples are optimized against one surrogate model. This is similar to solving problem (1) in a deterministic way by approximating the expectation of the predictive posterior with a “plug-in” estimation of the parameters, $\hat{\theta}_{\text{MAP}}$ the maximum a posteriori probability (MAP) estimate: $\delta^* \approx \delta_{\hat{\theta}_{\text{MAP}}}$. To avoid overfitting to the surrogate model, random transformations of inputs or prediction function were developed in the literature (see Section 2).

Our contribution lies into the use of *approximate Bayesian inference as surrogate in black-box adversarial attack*. We replace the crude MAP approximation of the predictive posterior distribution by a more accurate one to generate transferable adversarial examples. Therefore, we focus on the training phase by considering the methods and the computational costs of obtaining the surrogate model, whereas most previous work searches to optimize adversarial examples crafting at the time of the attack (“test time”).

SG-MCMC & cSGLD. In practice, we approximate the posterior $p(\theta|\mathcal{D})$ by the ensemble of the samples obtained from Stochastic Gradient-Markov Chain Monte Carlo (SG-MCMC). SG-MCMC is a family of optimization techniques, inaugurated by SGLD (Welling & Teh, 2011), that combines Stochastic Gradient Descent (SGD) with MCMC. By adding noise during training, it allows us to sample from the posterior distribution of parameters. Our method aims to solve the following optimization problem:

$$\delta_{\{\theta_s\}} = \arg \min_{\|\delta\|_p \leq \varepsilon} \frac{1}{S} \sum_{s=1}^S \hat{p}(y|x + \delta, \theta_s) \quad (2)$$

where $\{\theta_s\}_{s=1}^S$ are samples of the model parameters.

We choose to apply the recently proposed *cyclical Stochastic Gradient Langevin Dynamics* (cSGLD) (Zhang et al., 2020), a state-of-the-art SG-MCMC technique. cSGLD divides the training in cycles that all start from the initial learning rate value (cf. illustration in supplementary materials). Each cycle is composed of (1) an exploration stage with larger learning rates which corresponds to the warmup period of MCMC algorithms; (2) a sampling stage that samples parameters at regular intervals and operates with smaller learning rates and added noise. cSGLD can be viewed as SG-MCMC with warm restarts. Starting a new cycle with a large learning rate allows the exploration of another local maximum of the loss landscape. cSGLD has the compelling advantage of sampling from both several modes of the posterior distributions on parameters and locally inside each mode. Ashukha et al. (2020) show that this technique produces one of the

best results among ensemble methods considering both the quality of the ensemble and the computational cost.

Extension to unknown architecture. Let $\mathcal{A} = \{a_i\}_i$ be a countable set of architectures, $p(a)$ a prior on \mathcal{A} , θ^a the parameters of the architecture a and $\hat{p}^a(y|x, \theta^a)$ its predictive distribution. Discarding the previous hypothesis (i) on the knowledge of the architecture, we can consider the architecture of the target a to be a random variable and the true predictive posterior distribution can be decomposed with the law of total expectation:

$$p(y|x, \mathcal{D}) = \mathbb{E}_{p(a)} \mathbb{E}_{p(\theta^a|\mathcal{D})} \hat{p}^a(y|x, \theta^a) \quad (3)$$

If \mathcal{A} is finite and small, we can approximate this quantity with a weighted average of one cSGLD predictive posterior approximation per architecture. More realistically, we sample according to $p(a)$ a finite subset $A = \{a_i \sim p(a)\}_{i=1}^{S_A} \subset \mathcal{A}$ of architectures where the number of architectures S_A is fixed by the computational budget. We sample S parameters $\{\theta_s^a\}_{s=1}^S$ for all $a \in A$. Then, our inter-architecture attack that minimizes our approximation of $p(y|x, \mathcal{D})$ becomes:

$$\delta_A = \arg \min_{\|\delta\|_p \leq \varepsilon} \frac{1}{|A|} \sum_{a \in A} \frac{1}{S} \sum_{s=1}^S \hat{p}^a(y|x + \delta, \theta_s^a) \quad (4)$$

Attack algorithm. One can approximate the solution of Equations 2 and 4 by applying existing adversarial attack algorithms with minor modifications. Thus, our method is a simple, effective and efficient way to improve the transferability of adversarial examples (as later revealed by our experiments). We adapted four popular iterative gradient-based attacks to accommodate the large number of models produced by cSGLD. Algorithm 1 exemplifies such adaptation for I-FG(S)M. This algorithm supports multiple cSGLD executions, which proves useful to generalize to multi-architectures attacks. We trained cSGLD once per architecture and at each iteration, we compute the gradient of the ensemble composed of one random sample of each Markov chain.

4. Experimental Protocol

4.1. Objectives and Research Questions

The goal of our approach is to increase the transferability of adversarial examples by using a surrogate ensemble of samples from the posterior distribution to attack a DNN. Since SG-MCMC methods sample the weights of a given architecture, we expect our approach to work particularly well in settings where the architecture of the target model is known, but not its weights. Our first research question investigates this and asks:

Algorithm 1 Variant of I-FG(S)M attack to operate on a large number of models from multiple architectures

Input: original example (x, y) , S_A ordered sets of model parameters $(\theta_s^1)_{s=1}^S, \dots, (\theta_s^{S_A})_{s=1}^S$, number of iterations n_{iter} , perturbation p -norm ε , step-size α

Output: adversarial example x_{adv}

Shuffle each ordered set of model samples $(\theta_s^1)_{s=1}^S, \dots, (\theta_s^{S_A})_{s=1}^S$

$x_{\text{adv}} \leftarrow x$

for $i = 1$ **to** n_{iter} **do**

$x_{\text{adv}} \leftarrow x_{\text{adv}} + \frac{\alpha}{S_A} \sum_{a=1}^{S_A} \nabla \mathcal{L}(x_{\text{adv}}; y, \theta_{i \bmod S}^a)$

$x_{\text{adv}} \leftarrow \text{project}(x_{\text{adv}}, B_\varepsilon[x])$

$x_{\text{adv}} \leftarrow \text{clip}(x_{\text{adv}})$

end for

RQ1: *Does our approach improve the intra-architecture transferability of adversarial attacks?*

To answer this question, we compare the transfer rates of four classical gradient-based attacks when applied from (i) an ensemble of models sampled using our cSGLD-based approach; (ii) a single surrogate trained for as many epochs; (iii) an ensemble of independently trained DNNs. The target DNN and surrogate models have the same architecture.

Next, we consider black-box settings where the architecture of the target model is unknown (and not used to build the surrogate model). Given that cSGLD sticks to sampling models from the same architecture, we expect it to perform less effectively. Therefore, we combine it with the principles of ensemble-based attack of Liu et al. (2017) to build an ensemble of models sampled from different architectures. Our second research question evaluates the effectiveness of this hybrid approach:

RQ2: *Can our approach be combined with ensemble-based attacks to improve inter-architecture transferability?*

To answer this question, we consider five model architectures. We hold out one of them to act as the target model. Then, we train with cSGLD the four remaining architectures (which act as surrogates) to sample the same number of models for each of them. We attack the resulting set of samples and measure the transfer rate on the target model. We compare this to the classical ensemble-based attack of Liu et al. (2017), applied on an ensemble formed by one DNN per surrogate architecture. Both approaches work with the same computational budgets for training and attacking.

Given that our approach works at training time, our next research question investigates if combining it with test-time techniques yields further improvements.

RQ3: *Can our approach be combined with test-time trans-*

formations to further improve transferability?

We answer this question by applying three test-time transformations designed for transferability to an ensemble of cSGLD samples and to an ensemble of independently trained DNNs obtained with at least the same number of epochs.

Finally, we study the impact of the number of cSGLD cycles on the effectiveness of our approach. Increasing the number of cycles enables sampling from different modes of the weight posterior distribution, yet at the cost of additional training epochs. We ask:

RQ4: *How does the number of cycles impact transfer rate?*

We answer this question by repeating the experimental protocol of RQ1 with different numbers of cycles.

4.2. General Experimental Setup

Datasets. We consider CIFAR-10 (Krizhevsky, 2009) and ImageNet (ILSVRC2012; Russakovsky et al. 2015). In all cases, we train the surrogate and target models on the entire training set. For each CIFAR-10 target model, we select all the examples from the test set that are correctly predicted by it. In the case of ImageNet, we use a random subset of 5000 correctly predicted test images.

Architectures. Following the work of Ashukha et al. (2020), we consider the following five architectures for CIFAR-10: PreResNet110, PreResNet164 (He et al., 2016b), VGG16BN, VGG19BN (Simonyan & Zisserman, 2015) and WideResNet28x10 (Zagoruyko & Komodakis, 2016). For ImageNet, we select five architectures with $3 \times 224 \times 224$ input size. Three classical architectures: ResNet-50 (He et al., 2016a)¹, ResNeXt-50 32x4d (Xie et al., 2017b) and Densenet-121 (Xie et al., 2017b); and 2 mobile architectures: MNASNet 1.0 (Tan et al., 2018) and EfficientNet-B0 (Tan & Le, 2019). In doing so, we cover a diverse set of architectures in terms of heterogeneity (similar and different families of architecture), computation cost, and release date.

Target models The target models are deterministic DNNs. In the case of CIFAR-10, they are trained using Adam optimizer for 250 epochs with step-wise learning rate decay that divides it by 10 every 75 epochs (the architecture depends on the experiments). For ImageNet, we use the pre-trained models provided by PyTorch (Paszke et al., 2019) and the pre-trained EfficientNet-B0 provided by PyTorch Image Models (*timm*). The benign accuracy of all target models exceeds 83% (CIFAR-10) and 73% (ImageNet); see supplementary materials for exact values.

Surrogate models (classical ensembles) For CIFAR-10,

¹Ashukha et al. (2020) study ResNet-50 only on ImageNet. We used their shared trained models as surrogate DNNs.

the DNNs used to form surrogate ensembles are trained using the same process as the target models. Therefore the comparison between deterministic DNNs and cSGLD is fair, since one can expect the deterministic DNNs surrogate to be “close” to the target. As for ImageNet, we retrieve an ensemble of 15 ResNet-50 models trained independently by Ashukha et al. (2020) using SGD with momentum during 130 epochs. For the RQ2 experiments, we train similarly one model for every 4 other ImageNet architectures.

Surrogate models (cSGLD). Following the work of Ashukha et al. (2020) and Zhang et al. (2020), we train models with cSGLD for 5 learning rate cycles (which, as our RQ4 experiments reveal, is where the transfer rate starts plateauing), except for the RQ2 experiments on ImageNet where we used 3 cycles due to computational limitations. The learning rate is set with cosine annealing schedule for fast convergence. Each cycle lasts 50 epochs on CIFAR-10 and 45 on ImageNet. The last 3 epochs of every cycle form the sampling phase: noise is added and one sample is drawn at the end of each epoch. Therefore, we obtain 3 samples per cycle, and 15 samples in total. An illustration of a cSGLD cyclical learning rate schedule is in supplementary materials. To train ResNet-50 models on ImageNet, we re-use the same hyperparameters for cSGLD than Ashukha et al. (2020) used for snapshot ensembles.

Adversarial attacks. We applied our variant of 4 gradient-based attacks as described previously. The attacker’s goal is misclassification (untargeted adversarial examples). We perform both 2-norm and ∞ -norm bounded adversarial attacks. In accordance to values commonly used in the literature (Croce & Hein, 2020), the maximum perturbation norm ϵ is set respectively to 0.5 and $\frac{4}{255}$ on CIFAR-10, and respectively to 3 and $\frac{4}{255}$ on ImageNet. The step-size α is set to $\frac{\epsilon}{10}$. We choose to perform 50 iterations such that the transferability rates plateaus for all iterative attacks (I-FGSM, MI-FGSM and PGD) on both norms and both datasets (see supplementary materials). PGD runs with 5 random restarts. Unless otherwise stated, every iteration computes the gradient of 1 model per architecture. The unique FG(S)M gradient is computed against all available models. cSGLD samples are attacked in random order. The MI-FSGM decay factor is set to 0.9.

Test-time Transformations In RQ3, we consider three test-time transformations applied during attack designed for transferability (see Section 2): Ghost Networks (Li et al., 2018), Input Diversity (Xie et al., 2019) and Translation Invariant (Dong et al., 2019). We implemented them in PyTorch with their original hyperparameters. To extend Input Diversity to the smaller input sizes of CIFAR-10, we keep the same maximum resize ratio of 0.9.

Implementation. The source code and trained models of

Dataset	Surrogate	L2 Attack	L ∞ Attack	Nb epochs
CIFAR-10	cSGLD	93.46 %	93.42 %	250
	1 DNN	49.02 %	77.96 %	250
	2 DNNs	57.41 %	85.20 %	500
	5 DNNs	63.53 %	94.98 %	1250
	15 DNNs	66.45 %	98.02 %	3750
ImageNet	cSGLD	94.94 %	90.82 %	225
	1 DNN	65.52 %	57.94 %	130
	2 DNNs	81.34 %	75.06 %	260
	5 DNNs	94.96 %	93.32 %	650
	15 DNNs	98.62 %	98.46 %	1950

Table 1. Intra-architecture transfer rates of I-FG(S)M with 50 iterations. Higher is better.

Dataset	Surrogate	L2 Attack	L ∞ Attack	Nb epochs
CIFAR-10	cSGLD	93.45 %	94.85 %	250
	1 DNN	74.53 %	81.01 %	250
	2 DNNs	85.54 %	90.91 %	500
	5 DNNs	92.76 %	97.24 %	1250
	15 DNNs	94.74 %	98.36 %	3750
ImageNet	cSGLD	94.26 %	94.04 %	225
	1 DNN	61.40 %	63.46 %	130
	2 DNNs	78.42 %	80.08 %	260
	5 DNNs	94.82 %	95.58 %	650
	15 DNNs	98.98 %	99.22 %	1950

Table 2. Intra-architecture transfer rates of MI-FG(S)M with 50 iterations. Higher is better.

the experiments are publicly available on GitHub². Our attack is built on top of the Python ART library (Nicolae et al., 2018). cSGLD models were trained thanks to the implementation of Ashukha et al. (2020) available on GitHub³. cSGLD and DNNs models were trained with PyTorch (Paszke et al., 2019). We use EfficientNet-B0 from timm⁴.

Infrastructure. CIFAR-10 experiments were run on NVIDIA Tesla V100-SXM2-16G GPUs, and ImageNet experiments on NVIDIA Tesla V100-DGXS-32GB GPUs.

5. Experimental Results

5.1. RQ1: Intra-architecture transferability

We compare the intra-architecture transfer rate achieved by our approach (using cSGLD) with the classical ensemble-

²<https://github.com/framartin/transferable-bnn-adv-ex>

³<https://github.com/bayesgroup/pytorch-ensembles>

⁴<https://github.com/rwightman/pytorch-image-models>

Dataset	Attack	Norm	T-DEE	Comput. Ratio
CIFAR-10	I-FG(S)M	L2	>15	>15
		L ∞	3.80	3.80
	MI-FG(S)M	L2	6.08	6.08
		L ∞	2.98	2.98
	PGD	L2	>15	>15
		L ∞	4.00	4.00
ImageNet	FG(S)M	L2	>15	>15
		L ∞	7.35	7.35
	I-FG(S)M	L2	4.93	2.85
		L ∞	4.18	2.42
	MI-FG(S)M	L2	4.83	2.79
		L ∞	4.39	2.54
PGD	L2	4.90	2.83	
	L ∞	4.25	2.46	
FG(S)M	L2	5.31	3.07	
	L ∞	6.16	3.56	

Table 3. Number of DNNs (T-DEE) and computation budget (Comput. Ratio, measured as number of epochs) needed to achieve the same intra-architecture transferability than cSGLD using classical deep ensemble. Higher is better. “>15” indicates that 15 DNNs have a lower transfer rate than cSGLD.

based method (using 1, 2, 5 and 15 DNNs). The used architectures are PreResNet110 (CIFAR-10) and ResNet-50 (ImageNet). Tables 1 and 2 show the transfer rates. Due to lack of space, we only show detailed results for I-FG(S)M and MI-FG(S)M; results for PGD and FG(S)M are provided as supplementary materials and discussed below as well.

Overall, our approach achieves a transfer rate of at least 88.90% when combined with I-FGSM, MI-FGSM or PGD; and between 44.85% and 67.72% for FGSM. At a similar computation cost (number of epochs), it systematically increases the transfer rate by 12.76 (ImageNet, FG(S)M, L2) to 44.44 (CIFAR-10, I-FG(S)M, L2) percentage points. One explanation for the highest improvements is that classical ensemble attacks using L2 norm suffer from the zero gradient phenomenon, whereas cSGLD avoids it because fast convergence and warm restarts prevent global convergence.

Table 3 provides another view on the results. Inspired by the DEE metric (Ashukha et al., 2020), we define the *Transferability-Deep Ensemble Equivalent (T-DEE)* metric as the number of independently trained DNNs needed to achieve the same transfer rate as cSGLD (computed with linear interpolation). We also report the *computing ratio*, i.e., the number of epochs of such DNNs ensemble divided by the number of epochs used to trained cSGLD. It represents the computational gain factor (expressed as the number of training epochs) achieved by our approach, which is different from T-DEE in the ImageNet case, since the DNNs are trained for 130 epochs while cSGLD uses 225 epochs.

On both datasets, the cSGLD surrogate always yields a higher transfer rate than an ensemble of 3 surrogate DNNs while requiring, in the worst case, 2.42 times fewer training epochs. On CIFAR-10 and considering L2 attack specifically, it even outperforms the ensemble of 15 DNNs by a significant factor (up to 27.01 percentage points). On ImageNet, the cSGLD surrogate achieves the same transfer rate as 4.18–6.16 DNNs, which corresponds to dividing the number of epochs by a factor between 2.42 and 3.56.

We conclude that cSGLD meaningfully and efficiently exploits parameter uncertainty and that this uncertainty is useful to discover generic adversarial directions. The increased transferability at constant computational cost emphasizes the benefits that one can gain from the cyclical nature of cSGLD, thanks to warm restarts, fast convergence, and the local characterization of each mode of the parameters posterior.

5.2. RQ2: Inter-architecture transferability

We study inter-architecture transferability, using the I-FGSM attack. Applying Algorithm 1, at each iteration we attack an ensemble comprising one sample of each of the four surrogate architecture. Then we evaluate the transfer rate on a deterministic DNN of the fifth (hold out) architecture. We repeat this experiment once for each hold-out architecture and compare with the classical ensemble comprising one DNN per surrogate architecture. Given the computational cost involved in training different architectures, the training processes are limited to 135 epochs for ImageNet (for cSGLD, this means 3 cycles of 45 epochs).

As shown in Tables 4 (CIFAR-10) and 5 (ImageNet), our method systematically and significantly improved transferability on all 5 hold-out architectures for both CIFAR-10 and ImageNet at constant train and attack cost. On CIFAR-10, the differences ranges from 11.6 to 25.8 percentage points for the 2-norm constraint, and from 2.5 to 10.5 for the ∞ -norm constraint. Our method even performs better than 4 DNNs per architecture for the L2 attack, despite training for 4 times fewer epochs. On ImageNet, the cSGLD surrogates improve over the single DNN counterpart by 11.8 and 29.2 percentage points of transfer rate at constant computational train and attack budget.

We conclude that our method can improve transferability even when the target architecture is unknown. This tends to indicate that the adversarial directions against posterior predictive distribution are partially aligned across different architectures. In other words, given a common classification task, there might exist a part of the uncertainty in parameters’ estimate that is common across architectures, and the variability of one architecture’s parameters might be informative of the variability of parameters of another architecture.

5.3. RQ3: Test-time transferability techniques

We study the transfer rates of I-FG(S)M (with 50 iterations) on the same architecture improved by three test-time techniques to improve transferability. Each technique is applied twice: on cSGLD with 15 samples (5 cycles \times 3 samples) and on DNN ensembles (1 DNN for CIFAR-10, 2 for ImageNet). I-FG(S)M computes the same number of gradients per iteration in both cases (1 for CIFAR-10, 2 for ImageNet). Thus, every attack performs a total of 50 backward passes on CIFAR-10 and 100 ones on ImageNet.

Note that since Translation Invariant is designed to increase transferability against a defended target model, we evaluated it against one of the studied defenses Xie et al. (2017a) applied to our target DNN. Thus, its transferability cannot be compared to the baseline or other test-time techniques.

Table 6 shows the results. We observe that our approach and the test-time techniques complement well to each other. Indeed, the transfer rates achieved by each test-time technique is further increased (by up to 25.1 percentage points) when applied on the cSGDL surrogate compared to classical DNNs (single or ensemble) trained for the same (or a higher) number of epochs. In particular, our results corroborate those of Li et al. (2018) as cSGDL allows increasing the number of “base models” used by Ghost Networks. On the other side, since cSGLD approximates the parameters posterior with a few samples, it benefits from the ability of test-time transformations to avoid overfitting to specific models in order to find general adversarial directions.

5.4. RQ4: Hyperparameters

Figure 1 shows the impact of the number of cycles on the transfer rate. The increase is substantial from one to two cycles (from 72.05% to 86.84% for L2 and from 74.80% to 87.62% for L ∞). The increase continues with more cycle before plateauing at 5–6 cycles. This reveals that exploring modes of the parameters posterior plays an important role to generate transferable adversarial examples and that there is some local geometric diversity of the loss landscape among local maximums.

The marginal impact beyond 6 cycles becomes noisy. We hypothesize that this due to the limits of cSGLD (inherent to warm restarts), which produces correlated samples. Thus, an interesting direction is to investigate the use of multiple runs of cSGLD to improve intra-architecture transferability.

6. Conclusion

We propose the first method that uses Bayesian neural networks as a surrogate in transfer-based adversarial attacks. We show that attacking the Bayesian approximate predictive posterior distribution is an efficient and effective way

Efficient and transferable adversarial examples from Bayesian Neural Networks

Attack	Surrogate	–PreResNet110	–PreResNet164	–VGG16bn	–VGG19bn	–WideResNet	Nb epochs
L2	1 cSGLD per arch.	96.20 %	96.34 %	56.74 %	53.56 %	87.70 %	4 × 250
	1 DNN per arch.	70.44 %	71.35 %	42.16 %	42.00 %	68.91 %	4 × 250
	4 DNNs per arch.	79.36 %	79.26 %	51.51 %	51.26 %	80.26 %	4 × 1000
L ∞	1 cSGLD per arch.	96.84 %	97.07 %	59.73 %	55.73 %	88.48 %	4 × 250
	1 DNN per arch.	88.25 %	90.30 %	55.99 %	53.25 %	77.97 %	4 × 250
	4 DNNs per arch.	96.75 %	97.36 %	66.82 %	66.06 %	90.06 %	4 × 1000

Table 4. Transfer rates of I-FG(S)M attack with 50 iterations on CIFAR-10 hold-out architectures. Higher is better.

Attack	Surrogate	–ResNet50	–ResNeXt50	–DenseNet121	–MNASNet	–EfficientNetB0	Nb epochs
L2	1 cSGLD per arch.	93.36 %	90.84 %	92.36 %	96.06 %	81.78 %	4 × 135
	1 DNN per arch.	73.58 %	72.40 %	65.40 %	84.22 %	54.70 %	4 × 135
L ∞	1 cSGLD per arch.	92.42 %	89.66 %	91.00 %	96.02 %	79.82 %	4 × 135
	1 DNN per arch.	70.14 %	69.12 %	61.76 %	82.28 %	50.62 %	4 × 135

Table 5. Transfer rates of I-FG(S)M attack with 50 iterations on ImageNet hold-out architectures. Higher is better.

Dataset	Test-time Transformation	Base model	L2 Attack	L ∞ Attack	Nb epochs	Nb backwards
CIFAR-10	Ghost Networks	cSGLD	95.29 %	94.54 %	250	50
		1 DNN	83.67 %	80.41 %	250	50
	Input Diversity	cSGLD	94.55 %	94.58 %	250	50
		1 DNN	69.42 %	85.15 %	250	50
	Translation Invariant	cSGLD	22.42 %	21.03 %	250	50
		1 DNN	17.28 %	18.87 %	250	50
Baseline (None)	cSGLD	93.46 %	93.42 %	250	50	
	1 DNN	49.02 %	77.96 %	250	50	
ImageNet	Ghost Networks	cSGLD	98.06 %	96.92 %	225	100
		2 DNNs	96.08 %	93.46 %	260	100
	Input Diversity	cSGLD	98.08 %	97.12 %	225	100
		2 DNNs	95.60 %	94.36 %	260	100
	Translation Invariant	cSGLD	61.68 %	56.86 %	225	100
		2 DNNs	45.46 %	43.42 %	260	100
Baseline (None)	cSGLD	95.54 %	93.54 %	225	100	
	2 DNNs	84.88 %	80.58 %	260	100	

Table 6. Transfer rates of I-FG(S)M attack (with 50 iterations) improved by our approach combined with test-time transformations.

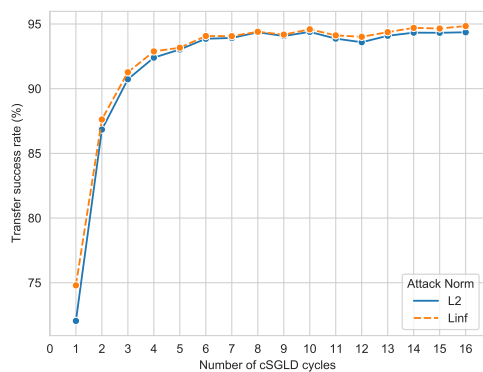


Figure 1. Intra-architecture transfer rate with respect to the number of cSGLD cycles. I-FG(S)M is performed with 50 iterations.

to craft adversarial examples transferable to deterministic neural networks. Our approach can be combined effectively with existing adversarial attacks, as one can use it on top of them to generate diverse sets of models efficiently and with minor modifications. Our experimental results demonstrate its benefits in increasing intra- and inter-architecture transferability compared to classical ensemble-based attacks. Moreover, one can combine it with test-time transformations to improve transferability even further. Overall, we provide new evidence that the Bayesian framework is a promising research direction for adversarial machine learning.

References

- Ashukha, A., Lyzhov, A., Molchanov, D., and Vetrov, D. Pitfalls of In-Domain Uncertainty Estimation and Ensembling in Deep Learning. 2 2020. URL <http://arxiv.org/abs/2002.06470>.
- Biggio, B., Corona, I., Maiorca, D., Nelson, B., Šrđić, N., Laskov, P., Giacinto, G., and Roli, F. Evasion attacks against machine learning at test time. In *Lecture Notes in Computer Science (including subseries Lecture Notes in Artificial Intelligence and Lecture Notes in Bioinformatics)*, volume 8190 LNAI, pp. 387–402, 8 2013. ISBN 9783642409936. doi: 10.1007/978-3-642-40994-3_{_}25. URL <http://arxiv.org/abs/1708.06131>http://dx.doi.org/10.1007/978-3-642-40994-3_25.
- Carbone, G., Wicker, M., Laurenti, L., Patane, A., Bortolussi, L., and Sanguinetti, G. Robustness of Bayesian Neural Networks to Gradient-Based Attacks. *arXiv*, 2 2020. URL <http://arxiv.org/abs/2002.04359>.
- Che, Z. A New Ensemble Adversarial Attack Powered by Long-Term Gradient Memories. pp. 3405–3413, 2020. URL <https://aaai.org/ojs/index.php/AAAI/article/view/5743>.
- Croce, F. and Hein, M. Reliable evaluation of adversarial robustness with an ensemble of diverse parameter-free attacks. 3 2020. URL <http://arxiv.org/abs/2003.01690>.
- Dargan, S., Kumar, M., Ayyagari, M. R., and Kumar, G. A Survey of Deep Learning and Its Applications: A New Paradigm to Machine Learning. *Archives of Computational Methods in Engineering*, 27(4):1071–1092, 9 2019. ISSN 18861784. doi: 10.1007/s11831-019-09344-w. URL <https://link.springer.com/article/10.1007/s11831-019-09344-w>.
- Dong, Y., Liao, F., Pang, T., Su, H., Zhu, J., Hu, X., and Li, J. Boosting Adversarial Attacks with Momentum. In *Proceedings of the IEEE Computer Society Conference on Computer Vision and Pattern Recognition*, pp. 9185–9193, 10 2018. ISBN 9781538664209. doi: 10.1109/CVPR.2018.00957. URL <http://arxiv.org/abs/1710.06081>.
- Dong, Y., Pang, T., Su, H., and Zhu, J. Evading defenses to transferable adversarial examples by translation-invariant attacks. In *Proceedings of the IEEE Computer Society Conference on Computer Vision and Pattern Recognition*, volume 2019-June, pp. 4307–4316, 4 2019. ISBN 9781728132938. doi: 10.1109/CVPR.2019.00444. URL <http://arxiv.org/abs/1904.02884>.
- Goodfellow, I. J., Shlens, J., and Szegedy, C. Explaining and Harnessing Adversarial Examples. 12 2014. URL <http://arxiv.org/abs/1412.6572>.
- Grosse, K., Pfaff, D., Smith, M. T., and Backes, M. The Limitations of Model Uncertainty in Adversarial Settings. 12 2018. URL <http://arxiv.org/abs/1812.02606>.
- Guo, Y., Li, Q., and Chen, H. Backpropagating Linearly Improves Transferability of Adversarial Examples. Technical report, 2020. URL <https://github.com/qizhangli/linbp-attack>.
- He, K., Zhang, X., Ren, S., and Sun, J. Deep residual learning for image recognition. In *Proceedings of the IEEE Computer Society Conference on Computer Vision and Pattern Recognition*, volume 2016-Decem, pp. 770–778. IEEE Computer Society, 12 2016a. ISBN 9781467388504. doi: 10.1109/CVPR.2016.90. URL <http://image-net.org/challenges/LSVRC/2015/>.
- He, K., Zhang, X., Ren, S., and Sun, J. Identity Mappings in Deep Residual Networks. *Lecture Notes in Computer Science (including subseries Lecture Notes in Artificial Intelligence and Lecture Notes in Bioinformatics)*, 9908 LNCS:630–645, 3 2016b. URL <http://arxiv.org/abs/1603.05027>.
- Huang, Q., Katsman, I., Gu, Z., He, H., Belongie, S., and Lim, S. N. Enhancing adversarial example transferability with an intermediate level attack. In *Proceedings of the IEEE International Conference on Computer Vision*, volume 2019-October, pp. 4732–4741, 7 2019. ISBN 9781728148038. doi: 10.1109/ICCV.2019.00483. URL <http://arxiv.org/abs/1907.10823>.
- Krizhevsky, A. Learning Multiple Layers of Features from Tiny Images. ... *Science Department, University of Toronto, Tech. ...*, 2009. ISSN 1098-6596. doi: 10.1.1.222.9220.
- Kurakin, A., Goodfellow, I. J., and Bengio, S. Adversarial examples in the physical world. In *5th International Conference on Learning Representations, ICLR 2017 - Workshop Track Proceedings*, 7 2019. URL <http://arxiv.org/abs/1607.02533>.
- Li, Y., Bai, S., Zhou, Y., Xie, C., Zhang, Z., and Yuille, A. Learning Transferable Adversarial Examples via Ghost Networks. *Proceedings of the AAAI Conference on Artificial Intelligence*, 34(07):11458–11465, 12 2018. ISSN 2374-3468. doi: 10.1609/aaai.v34i07.6810. URL <http://arxiv.org/abs/1812.03413>.

- Lin, J., Song, C., He, K., Wang, L., and Hopcroft, J. E. Nesterov Accelerated Gradient and Scale Invariance for Adversarial Attacks. 8 2019. URL <http://arxiv.org/abs/1908.06281>.
- Liu, Y., Chen, X., Liu, C., and Song, D. Delving into transferable adversarial examples and black-box attacks. *5th International Conference on Learning Representations, ICLR 2017 - Conference Track Proceedings*, 11 2017. URL <https://arxiv.org/abs/1611.02770><http://arxiv.org/abs/1611.02770>.
- Madry, A., Makelov, A., Schmidt, L., Tsipras, D., and Vladu, A. Towards deep learning models resistant to adversarial attacks. In *6th International Conference on Learning Representations, ICLR 2018 - Conference Track Proceedings*, 6 2018. URL <http://arxiv.org/abs/1706.06083>.
- Nicolae, M.-I., Sinn, M., Tran, M. N., Buesser, B., Rawat, A., Wistuba, M., Zantedeschi, V., Baracaldo, N., Chen, B., Ludwig, H., Molloy, I., and Edwards, B. Adversarial Robustness Toolbox v1.2.0. *CoRR*, 1807.01069, 2018. URL <https://arxiv.org/pdf/1807.01069>.
- Palacci, H. and Hess, H. Scalable Natural Gradient Langevin Dynamics in Practice. 6 2018. URL <http://arxiv.org/abs/1806.02855>.
- Papernot, N., McDaniel, P., and Goodfellow, I. Transferability in Machine Learning: from Phenomena to Black-Box Attacks using Adversarial Samples. 5 2016. URL <http://arxiv.org/abs/1605.07277>.
- Paszke, A., Gross, S., Massa, F., Lerer, A., Bradbury, J., Chanan, G., Killeen, T., Lin, Z., Gimelshein, N., Antiga, L., Desmaison, A., Kopf, A., Yang, E., DeVito, Z., Raison, M., Tejani, A., Chilamkurthy, S., Steiner, B., Fang, L., Bai, J., and Chintala, S. PyTorch: An Imperative Style, High-Performance Deep Learning Library. In Wallach, H., Larochelle, H., Beygelzimer, A., d'Alché-Buc, F., Fox, E., and Garnett, R. (eds.), *Advances in Neural Information Processing Systems* 32, pp. 8024–8035. Curran Associates, Inc., 2019. URL <http://papers.neurips.cc/paper/9015-pytorch-an-imperative-style-high-performance-deep-learning-library.pdf>.
- Russakovsky, O., Deng, J., Su, H., Krause, J., Satheesh, S., Ma, S., Huang, Z., Karpathy, A., Khosla, A., Bernstein, M., Berg, A. C., and Fei-Fei, L. ImageNet Large Scale Visual Recognition Challenge. *International Journal of Computer Vision (IJCV)*, 115(3):211–252, 2015. doi: 10.1007/s11263-015-0816-y.
- Simonyan, K. and Zisserman, A. Very deep convolutional networks for large-scale image recognition. In *3rd International Conference on Learning Representations, ICLR 2015 - Conference Track Proceedings*, 2015.
- Szegedy, C., Zaremba, W., Sutskever, I., Bruna, J., Erhan, D., Goodfellow, I., and Fergus, R. Intriguing properties of neural networks. 12 2013. URL <http://arxiv.org/abs/1312.6199>.
- Tan, M. and Le, Q. V. EfficientNet: Rethinking Model Scaling for Convolutional Neural Networks. *36th International Conference on Machine Learning, ICML 2019*, 2019-June:10691–10700, 5 2019. URL <http://arxiv.org/abs/1905.11946>.
- Tan, M., Chen, B., Pang, R., Vasudevan, V., Sandler, M., Howard, A., and Le, Q. V. MnasNet: Platform-Aware Neural Architecture Search for Mobile. *Proceedings of the IEEE Computer Society Conference on Computer Vision and Pattern Recognition*, 2019-June: 2815–2823, 7 2018. URL <http://arxiv.org/abs/1807.11626>.
- Wang, K. C., Vicol, P., Lucas, J., Gu, L., Grosse, R., and Zemel, R. Adversarial distillation of Bayesian neural network posteriors. In *35th International Conference on Machine Learning, ICML 2018*, volume 12, pp. 8239–8248, 6 2018. ISBN 9781510867963. URL <http://arxiv.org/abs/1806.10317>.
- Welling, M. and Teh, Y. W. Bayesian learning via stochastic gradient langevin dynamics. In *Proceedings of the 28th International Conference on Machine Learning, ICML 2011*, pp. 681–688, 2011. ISBN 9781450306195.
- Xie, C., Wang, J., Zhang, Z., Ren, Z., and Yuille, A. Mitigating Adversarial Effects Through Randomization, 11 2017a. URL <http://arxiv.org/abs/1711.01991>.
- Xie, C., Zhang, Z., Zhou, Y., Bai, S., Wang, J., Ren, Z., and Yuille, A. L. Improving transferability of adversarial examples with input diversity. In *Proceedings of the IEEE Computer Society Conference on Computer Vision and Pattern Recognition*, volume 2019-June, pp. 2725–2734, 3 2019. ISBN 9781728132938. doi: 10.1109/CVPR.2019.00284. URL <http://arxiv.org/abs/1803.06978>.
- Xie, S., Girshick, R., Dollár, P., Tu, Z., and He, K. Aggregated residual transformations for deep neural networks. In *Proceedings - 30th IEEE Conference on Computer Vision and Pattern Recognition, CVPR 2017*, volume 2017-Janua, pp. 5987–5995. Institute of Electrical and Electronics Engineers Inc., 11 2017b. ISBN 9781538604571. doi: 10.1109/CVPR.2017.634. URL <https://github.com/facebookresearch/ResNeXt>.

Zagoruyko, S. and Komodakis, N. Wide Residual Networks. *British Machine Vision Conference 2016, BMVC 2016, 2016-September:1–87, 5* 2016. URL <http://arxiv.org/abs/1605.07146>.

Zhang, R., Li, C., Zhang, J., Chen, C., and Wilson, A. G. Cyclical Stochastic Gradient MCMC for Bayesian Deep Learning. *International Conference on Learning Representations (ICLR), 2* 2020. URL <http://arxiv.org/abs/1902.03932>.

Supplementary Materials

In the supplementary materials for the paper, the following are provided:

- An illustration of the cSGLD cyclical learning rate schedule;
- A diagram of the relationships between gradient-based attacks;
- The natural accuracy of target Neural Networks;
- The proportions of 0-gradient of 1 cSGLD sample and of 1 DNN;
- The transfer rate of cSGLD with respect to the number of samples per cycle;
- The intra-architecture transfer rates computed in RQ1 on cSGLD and on ensembles of 1, 2, 5 and 15 DNNs with both 1 model per iteration and all available models per iteration;
- The transfer rate of iterative attacks with respect to the number of iterations;
- The train and attack hyperparameters used.

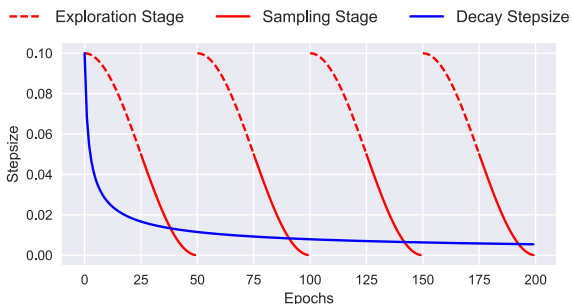


Figure 2. Illustration of the cSGLD cyclical learning rate schedule (red) and the traditional decreasing learning rate schedule (blue). Each cSGLD cycle is composed of an exploration phase (burn-in period of MCMC algorithms — red dotted) and of a sampling phase (red plain). Figure taken from Zhang et al. (2020).

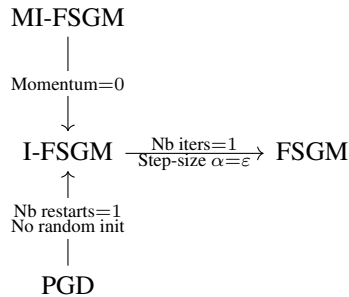


Figure 3. Relationships between gradient-based attacks.

Dataset	Target DNN	Benign Test Accuracy
CIFAR-10	PreResNet110	93.13 %
	PreResNet164	92.86 %
	VGG16bn	83.46 %
	VGG19bn	83.53 %
	WideResNet28x10	92.06 %
ImageNet	ResNet50	76.15 %
	ResNeXt50 32x4d	77.62 %
	Densenet121	74.65 %
	MNASNet 1.0	73.51 %
	EfficientNet-B0	77.70 %

Table 7. Top-1 accuracy on natural test examples for every target deterministic Neural Network.

Dataset	Surrogate Model	Proportion of 0-gradients
CIFAR-10	1 cSGLD sample	9.58 %
	1 DNN	65.43 %
ImageNet	1 cSGLD sample	0.24 %
	1 DNN	0.08 %

Table 8. Proportion of gradients with a L2 norm lower than 10^{-8} , the tolerance used by the library Adversarial Robustness Toolbox in L2 attacks to avoid division by 0 in norm scaling. Gradients are of the models of RQ1 (PreResNet110 for CIFAR-10, ResNet-50 for ImageNet) and on all the original examples of the test sets.

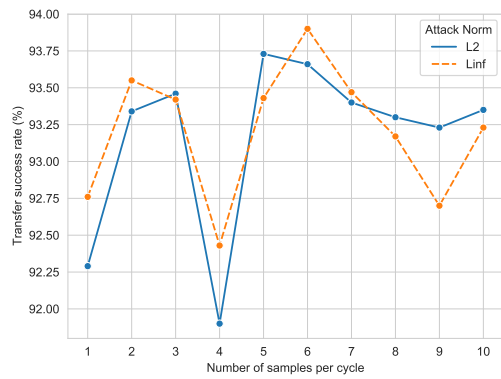


Figure 4. Transferability of adversarial examples with respect to the number of cSGLD samples per cycle. We trained one PreRes-Net110 cSGLD on CIFAR-10 for every number of cycles from 1 to 10 samples per cycle. Each additional sample per cycle increases the training cost by 1 epoch per cycle (5 epochs in total). A fixed number of 5 cSGLD cycles and 50 iterations of I-FG(S)M are used.

Dataset	Attack	Surrogate	L2 Attack	L_∞ Attack	Nb training epochs	Nb backward passes
CIFAR-10	I-FG(S)M	cSGLD	93.46 %	93.42 %	250	50
		1 DNN	49.02 %	77.96 %	250	50
		2 DNNs	57.41 %	85.20 %	500	50
		5 DNNs	63.53 %	94.98 %	1250	50
		15 DNNs	66.45 %	98.02 %	3750	50
	MI-FG(S)M	cSGLD	93.45 %	94.85 %	250	50
		1 DNN	74.53 %	81.01 %	250	50
		2 DNNs	85.54 %	90.91 %	500	50
		5 DNNs	92.76 %	97.24 %	1250	50
		15 DNNs	94.74 %	98.36 %	3750	50
	PGD (5 restarts)	cSGLD	92.81 %	93.06 %	250	250
		1 DNN	55.76 %	78.24 %	250	250
		2 DNNs	64.17 %	84.63 %	500	250
		5 DNNs	71.17 %	94.60 %	1250	250
		15 DNNs	73.73 %	97.49 %	3750	250
ImageNet	I-FG(S)M	cSGLD	94.94 %	90.82 %	225	50
		1 DNN	65.52 %	57.94 %	130	50
		2 DNNs	81.34 %	75.06 %	260	50
		5 DNNs	94.96 %	93.32 %	650	50
		15 DNNs	98.62 %	98.46 %	1950	50
	MI-FG(S)M	cSGLD	94.26 %	94.04 %	225	50
		1 DNN	61.40 %	63.46 %	130	50
		2 DNNs	78.42 %	80.08 %	260	50
		5 DNNs	94.82 %	95.58 %	650	50
		15 DNNs	98.98 %	99.22 %	1950	50
	PGD (5 restarts)	cSGLD	91.98 %	88.90 %	225	250
		1 DNN	58.06 %	54.10 %	130	250
		2 DNNs	74.54 %	71.26 %	260	250
		5 DNNs	92.46 %	91.94 %	650	250
		15 DNNs	97.96 %	97.76 %	1950	250

Table 9. Transfer rates of three gradient-based attacks on the same architecture (PreResNet110 for CIFAR-10, ResNet50 for ImageNet). Higher is better. cSGLD ensembles are composed of 15 models (5 cycles, 3 samples per cycle). Attacks (I-FG(S)M, MI-FG(S)M and PGD) are performed for 50 iterations. *Each iteration computes the gradient of a single model to keep the attack computational cost constant across ensemble sizes* (see Table 10 for attacks on all models at every iteration). FG(S)M is reported in Table 10 because the gradient of its unique iteration is computed on all available models

Dataset	Attack	Surrogate	L2 Attack	L_∞ Attack	Nb training epochs	Nb backward passes
CIFAR-10	I-FG(S)M	cSGLD	93.50 %	95.10 %	250	750
		1 DNN	49.45 %	77.93 %	250	50
		2 DNNs	50.31 %	90.78 %	500	100
		5 DNNs	49.04 %	97.48 %	1250	250
		15 DNNs	48.42 %	99.19 %	3750	750
	MI-FG(S)M	cSGLD	93.80 %	95.48 %	250	750
		1 DNN	74.72 %	80.98 %	250	50
		2 DNNs	83.87 %	91.93 %	500	100
		5 DNNs	87.90 %	97.82 %	1250	250
		15 DNNs	88.52 %	99.32 %	3750	750
	PGD (5 restarts)	cSGLD	93.44 %	95.31 %	250	3750
		1 DNN	56.33 %	78.27 %	250	250
		2 DNNs	58.23 %	91.15 %	500	500
		5 DNNs	56.74 %	97.56 %	1250	1250
		15 DNNs	55.84 %	99.25 %	3750	3750
	FG(S)M	cSGLD	44.85 %	60.11 %	250	15
		1 DNN	25.78 %	42.99 %	250	1
		2 DNNs	28.77 %	49.37 %	500	2
		5 DNNs	30.24 %	57.62 %	1250	5
		15 DNNs	31.25 %	64.05 %	3750	15
ImageNet	I-FG(S)M	cSGLD	95.20 %	94.42 %	225	750
		1 DNN	65.32 %	57.78 %	130	50
		2 DNNs	84.88 %	80.84 %	260	100
		5 DNNs	96.58 %	96.36 %	650	250
		15 DNNs	99.32 %	99.56 %	1950	750
	MI-FG(S)M	cSGLD	94.92 %	95.34 %	225	750
		1 DNN	61.56 %	64.10 %	130	50
		2 DNNs	82.46 %	84.52 %	260	100
		5 DNNs	96.22 %	97.24 %	650	250
		15 DNNs	99.28 %	99.54 %	1950	750
	PGD (5 restarts)	cSGLD	94.26 %	93.64 %	225	3750
		1 DNN	58.00 %	54.40 %	130	250
		2 DNNs	80.28 %	77.18 %	260	500
		5 DNNs	95.82 %	95.78 %	650	1250
		15 DNNs	99.28 %	99.46 %	1950	3750
	FG(S)M	cSGLD	58.66 %	67.72 %	225	15
		1 DNN	37.24 %	43.78 %	130	1
		2 DNNs	45.90 %	53.18 %	260	2
		5 DNNs	58.04 %	65.32 %	650	5
		15 DNNs	68.70 %	76.62 %	1950	15

Table 10. Transfer rates of three iterative gradient-based attacks on the same architecture (PreResNet110 for CIFAR-10, ResNet50 for ImageNet). Higher is better. cSGLD ensembles are composed of 15 models (5 cycles, 3 samples per cycle). Every attack is performed for 50 iterations. Contrary to Table 9, every iteration computes the gradient of all available models. Except for the L2 MI-F(S)GM on CIFAR-10, results are similar.

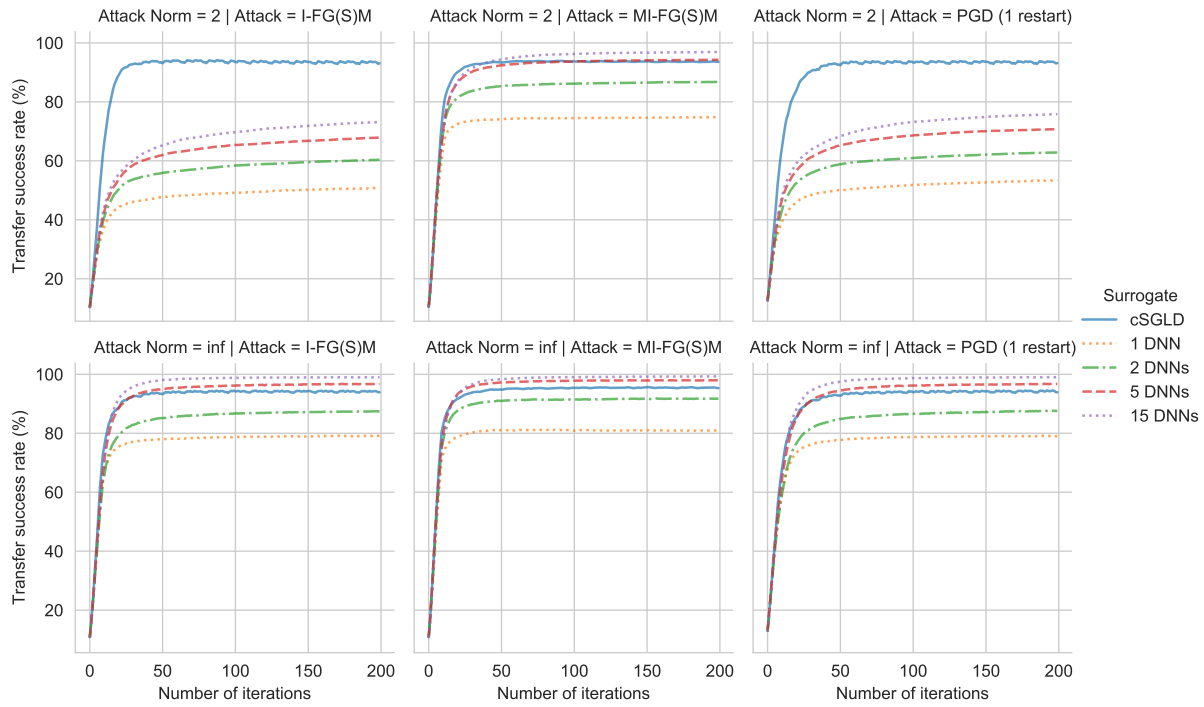


Figure 5. Transfer rates on CIFAR-10 of three iterative gradient-based attacks on the same architecture (PreResNet110) with respect to the number of iterations.

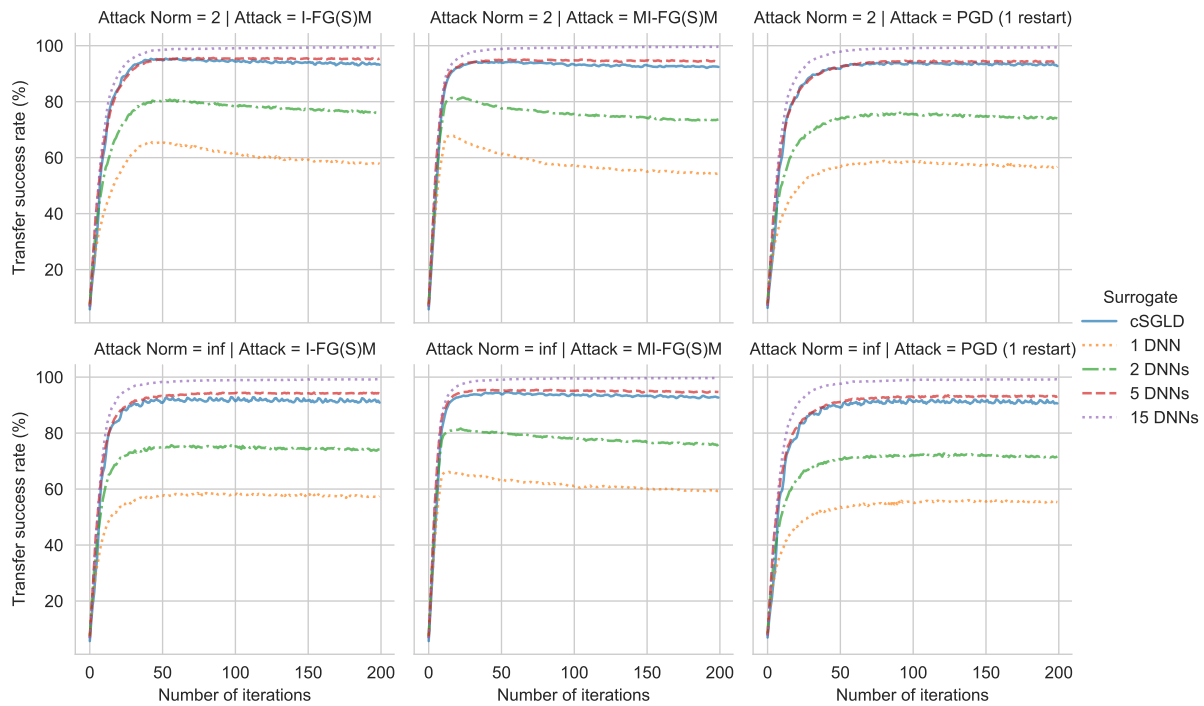


Figure 6. Transfer rates on ImageNet of three iterative gradient-based attacks on the same architecture (ResNet-50) with respect to the number of iterations.

Method	Hyperparameter	CIFAR-10			ImageNet	
		cSGLD	DNN Surrogate	DNN Target	cSGLD	DNN Surrogate
All	Number epochs	50 per cycle	250	250	45 per cycle	130 (135 for RQ2)
	Initial learning rate	0.5	0.01	0.01	0.1	0.1
	Learning rate schedule	Cosine Annealing	Step size decay ($\times 0.1$ each 75 epochs)	Step size decay ($\times 0.1$ each 75 epochs)	Cosine Annealing	Step size decay ($\times 0.1$ each 30 epochs)
	Optimizer	cSGLD	Adam	Adam	cSGLD	SGD
	Momentum	0	0.9	0.9	0.9	0.9
	Weight decay	5e-4 (3e-4 for PreResNet)	1e-4	1e-4	1e-4	1e-4
	Batch-size	64	128	128	256 for ResNet50, 64 for others	256 for ResNet50, 64 for others
cSGLD	Sampling interval	1 sample per epoch	-	-	1 sample per epoch	-
	Nb cycles	5	-	-	5 (3 for RQ2)	-
	Nb samples per cycle	3	-	-	3	-
	Nb epochs with noise	3	-	-	3	-

Table 11. Hyperparameters used to train cSGLD or deep ensemble Neural Networks. Target DNN on ImageNet is not included because it is retrieved from PyTorch pretrained models.

Attack / Technique	Hyperparameter	CIFAR-10	ImageNet
All attacks	Perturbation 2-norm ϵ	0.5	3
	Perturbation ∞ -norm ϵ	$\frac{4}{255}$	$\frac{4}{255}$
Iterative Attacks	Step-size α	$\frac{\epsilon}{10}$	$\frac{\epsilon}{10}$
	Number iterations	50	50
MI-FG(S)M	Momentum term	0.9	0.9
PGD	Number random restarts	5	5
Ghost Network	Skip connection erosion random range	[1-0.22, 1+0.22]	[1-0.22, 1+0.22]
Input Diversity	Minimum resize ratio	90 %	90 %
	Probability transformation	0.5	0.5
Translation Invariance	Kernel size	15	15

Table 12. Hyperparameters of attacks and test-time transferability techniques.